17th World Conference on Earthquake Engineering, 17WCEE
Sendai, Japan - September 13th to 18th 2020

Rationalization of Strain Limits for Dissipative Devices Used in Post-tensioned Rocking Structures

R. Liu[(1)], A. Palermo[(2)]

[(1)] *Post-doctoral Fellow, University of Canterbury New Zealand, royce.liu@canterbury.ac.nz*
[(2)] *Professor, University of Canterbury New Zealand, alessandro.palermo@canterbury.ac.nz*

Abstract

The post-tensioned rocking system also known as Dissipative Controlled Rocking (DCR) is a low damage structural system that uses dissipative devices for moment capacity and hysteretic damping. A commonly used family of replaceable dissipative devices for DCR are tension-compression metal hysteretic dissipaters made from mild steel. These devices are limited in cyclic capacity due to Low Cycle Fatigue (LCF) and maximum deformation capacity due to monotonic strain capacity of mild steel. Currently two design references suggest strain limits to be used with such dissipaters: 5% strain and 90% of the ultimate strain. These suggested values are wildly different and little reasoning or evidence provided to support the use of these values. This paper focusses on rationalizing the way in which strain limits for dissipaters should be proposed by showing that it should be selected based on the LCF capacity of the device, period of vibration of the structure, duration of the ground motion and number of dissipaters deemed acceptable to fail from LCF in an above design level earthquake. Response history analysis was undertaken on five modelled bridge piers at two limit states: design (Ultimate Limit State or Damage Control Limit State ULS/DCLS) and above design (Maximum Credible Earthquake or Collapse Avoidance Limit State MCE/CALS). The five bridge pier models were based on prototypes typical of NZ highway bridges and varied in properties and design drifts such that they covered a large range of possible effective periods of vibration. The dissipaters were designed to reach 5% strain at the design displacement of each model and used fatigue characteristics considered typical of mild steel. Modelling was undertaken in OpenSEES and the LCF damage received by the dissipaters were tracked. It was found that that, 5% design strain appears to be a reasonable value to use from the perspective of low cycle fatigue (LCF) capacity considering a single ULS or MCE level ground motion. The mean damage caused by short duration ULS motions were found to be around 12% and 26% for long duration motions. It was found that the mean and range of damage caused by long duration motions were dependent on the effective period of the structure and appear to be largest for structures of short effective period. In this study, the shortest period model (T_e=0.766s) received LCF damage ranging from 6-88% whereas the longest period model (Te = 2.07s) only received damage ranging between 9-36%. Cycling at the design strain was found not to be the major contributor to total LCF damage for a given dissipater. Furthermore, the results indicate that damage contribution as a function of cycling within particular strain bins appears to be random. It was found that long duration motions cause more LCF damage than short duration motions at both ULS and MCE. However, the direct correlation between duration and expected LCF damage was found to be weak due to significant scatter in observed LCF damage. At MCE both long and short duration motions resulted in dissipater fracture due to LCF. The mean percentage of dissipater layers fractured due to LCF by an MCE motion was found to be 46%.

Keywords: post-tensioned; rocking; strain-limits; low cycle fatigue; dissipative devices

1. Introduction

Post-tensioned rocking construction, also known as Dissipative Controlled Rocking (DCR), is a low structural damage alternative to conventional construction. It consists of making a structure articulated by inserting rocking joints at the interface of structural members (e.g. beam-column and column-foundation) and clamping the members together by stressed unbonded post-tensioning. In these structures, member plastic hinging is replaced by gap opening at the rocking joints and energy dissipation is isolated to components known as dissipative devices that are attached (either internal or external to the section) across the rocking interface. The simplest dissipative device that can be used internal to the section of the rocking member are rebar with a debonded zone. The simplest external dissipative devices consist of a machined steel rod with a section of reduced cross-sectional area (known as the fuse section) that is surrounded by anti-buckling componentry. Examples of the second device are the epoxy/grouted buckling restrained fuse dissipaters [1] and the grooved dissipater [2]. Both types of devices rely on tension-compression plastic deformation of steel.

DCR was initially developed for concrete buildings [3], [4] but since then, many different aspects of this construction scheme has been researched: application to bridges [5]–[10], application to steel buildings [11], [12], application to timber construction [13]–[15], use of different dissipative devices [1], [16]–[19], use of high performance materials [10], [20], [21], etc. An aspect which has received little attention is the prescription of design strain limits for dissipative devices suitable for post-tensioned rocking structures. Design strain limits for dissipative devices are important because they are a simple means of accounting for phenomena such as limited cyclic life (due to low cycle fatigue) and limited peak strain capacity (due to material ultimate strain). Although design strain limits are fundamentally device-specific due to material, construction, and mode of operation (e.g. tension-compression, torsion, etc) general strain limits can still be proposed, given, that they apply to a specific class of dissipative devices (e.g. tension-compression yielding) and that the design of those devices satisfies the assumptions used to obtain those limits. This paper limits its scope to tension-compression yielding dissipaters with section of reduced cross-sectional area made from AS/NZS 4671 Grade 300 mild steel or reinforcing steel of similar mechanical properties.

Two major design references which specify design strain limits for tension-compression yielding steel dissipaters are: the PRESSS Handbook and Appendix B of NZS3101:2006. The PRESSS handbook recommends a design strain of 5% for AS/NZS 4671:2001 Grade 300 steel whilst Appendix B of NZS3101:2006 recommends a maximum of 90% of the ultimate tensile strain. Little if any commentary to support the choice of these values exist in either reference. The strain limit suggested in Appendix B is clearly unconservative as it does not consider premature fracture due to buckling, fracture due to low cycle fatigue, or provision of reserve strain capacity for the dissipaters to be able to accommodate demands from above design level seismic loads.

Research into low cycle fatigue [22]–[28] and earthquake duration effects [29]–[31] on conventional reinforced concrete construction is pertinent and draws parallels to the research presented in this paper, however, there are several key differences. Here, inelastic strains are limited to the section of reduced cross-sectional area of the dissipative device and is governed by the elongation of the device and the length of the fuse section. This is in contrast to conventional construction where the system is more complex in the inelastic range (due to effects such as bond-slip relationship, strain penetration, tension- shift, spalling, bar buckling, etc.) making it difficult to even accurately ascertain the strain in any part of the reinforcing bar within the plastic hinge zone. It is assumed that the dissipaters are attached by relatively rigid brackets so that the effect of slip can be ignored, first mode buckling of the fuse section is prevented by anti-buckling componentry; and degradation of the reinforced concrete rocking member due to spalling is prevented by use of steel armoring.

Low cycle fatigue (LCF) is the phenomenon whereby metal components fracture, in less than a few hundred cycles, when they are subjected to load cycling within the inelastic range. The relationship between cyclic loading at a constant strain-amplitude (ε_a) and the corresponding number of cycles to failure N_f are commonly modelled by a power function of the form given by Eq. (1). This is colloquially known as the Coffin-Manson equation. In conjunction with Eq. (1), the Palmgren-Miner damage rule Eq. (2) is used to quantify the damage caused by a particular set of strain-amplitude cycles within a given loading history.

$$\epsilon_a = \epsilon_0' \left(2N_f\right)^m \quad (1)$$

$$D = \sum_{i=1}^{k} \frac{n_i}{N_i} \leq 1 \quad (2)$$

With respect to Eq. (1), cyclic testing on metal components are conducted to determine the constants ε_a and m. Multiple studies have been conducted so far to determine these constants for reinforcing steel such as Mander [24]. A limitation of these tests is the fact that they are material behavior tests (due to the very short gauge length), meaning, that the results obtained may not be directly applicable on the component scale, say a dissipative device made from the same steel, due to the occurrence of stress raisers such as geometry, higher mode/small scale buckling, etc. Likewise, many steel tension-compression dissipative devices have been developed and tested (epoxied/grouted buckling restrained fuse dissipater [1], [32], grooved dissipater [2], [19], bamboo dissipater [19], [33]), however, most of the tests have been conducted using variable amplitude loading protocols and therefore lack the rigour of LCF specific studies which directly link the number of cycles to failure to a given strain amplitude.

2. Aim and Methodology

The aim of this study was to investigate whether the design strain limit (5% strain) proposed by the PRESSS handbook is a reasonable value to use. This question itself is extremely broad and difficult to answer due to the complex entanglement of variables that includes: ground motion record characteristics, site distance effects, site soil conditions, effective period of the structure, low cycle fatigue properties of the dissipaters, etc. Furthermore, implications such as the impact which the design strain limit has on performance and collapse potential in a beyond design event must also be considered.

The approach taken in this study was to undertake parametric Non-Linear Response History Analyses (NLRHA) of Single Degree of Freedom (SDOF) DCR bridge piers at two limit states: the design point also called the Ultimate Limit State (ULS) and the Maximum Credible Earthquake (MCE). The rational of this approach was twofold. First, to have as wide a combination of structural dynamic properties and ground motion properties in order to ascertain the range of low cycle fatigue demands that could be imposed in a design level earthquake. Second, to ascertain implied performance in a beyond design level earthquake event, which here is considered to be the MCE. In each simulation, the displacement and LCF related damage of the dissipaters were recorded. The scope of this numerical study can be summarized as follows.

- Five SDOF bridge pier computer models covering a range of pier sizes and deck spans typically used in New Zealand were constructed. The pier models had different design drifts so that a range of effective period of vibrations could be covered.
- The models were assumed to be far-field structures (greater than 20km from surface faulting) and situated on NZS1170.5 Class C soil (Vs30 300-600ms-2 and soil depth ≤ 60m).
- External tension-compression dissipaters with controllable fuse length and fixed low cycle fatigue characteristics were assumed.
- For all models, the dissipaters were designed to reach 5% strain at ULS.

In the rest of this paper the limit states are referred to as the Damage Control Limit State (DCLS) and Collapse Avoidance Limit State (CALS). This terminology was used to be coherent with language used in the New Zealand Transport Agency design guidance document: Bridge Manual [34]. An important point of note, is that CALS is not quite the same as MCE because it is defined to be a seismic demand 1.5 times that of DCLS instead of the seismic demand arising from a ground motion of 2500 year return period.

3. Numerical Study

3.1 Prototype structures

Three prototype structures were used in this study (Table 1). The dimensions of these prototypes were chosen based on the range of commonly used bridge dimensions and deck types used in New Zealand. In terms of ground conditions and seismic hazard, the prototype structures were assumed to be constructed on Site Class C soil (as per NZS1170.5 definition) in an area of moderate seismicity (Z=0.3) and not be subject to near fault effects (N=1). The prototype bridges were assumed to be Importance Level 2 structures resulting in a return period factor of R=1.3.

Table 1 – Properties of the prototype structures.

	Prototype 1	**Prototype 2**	**Prototype 3**
Deck type and number of lanes	2-I beams, one lane	4-I beams, two lane	5-Super T, two lane
Span length (m)	20	20	30
Effective height (m)	4	6	8
Column diameter (m)	1.5	1.5	1.8
Seismic weight (kN)	1280	2655	4621

3.2 Displacement Based Design

Displacement based design was used to undertake the seismic design of the bridge piers based on the prototype structures. Three different design drifts were chosen (0.015, 0.02, 0.025 m/m) resulting in 9 potential designs. Preliminary calculations showed that some of these designs would have similar effective periods of vibration at the design displacement. The designs with similar periods of vibration were discarded resulting in 5 designs (labelled 1a, 2a, etc.) modelled in this study (Table 2).

Table 2 – Properties of the model structures.

	Prototype 1	**Prototype 2**		**Prototype 3**	
Design Model prefix	1a	2a	2b	3b	3c
Design drift (DCLS) θ_d	0.015	0.015	0.02	0.02	0.025
Design Base Shear kN	536	1042	791	1194	871
CALS drift θ_{CALS}	0.027	0.0245	0.035	0.031	0.041
Dissipater strain @ CALS drift	0.093	0.097	0.095	0.084	0.087
Post-tensioning: Initial post-tensioning (kN), Unbonded length (m), Area (mm^2)	534, 6.7, 1963	2393, 4, 12555	1100, 6.1, 3926	1947, 7.5, 12555	690, 8.1, 4185
Dissipaters: number, fuse area (mm^2), fuse length (mm)	8, 284.5, 390	12, 614, 240	12, 400, 430	12, 661, 457	12, 490, 685
Drift at first yield	0.00125	0.00265	0.00235	0.00275	0.00275

3.3 Ground motion selection

Ground motion records were obtained from two databases (PEER NGA West2, and KiK-net/K-NET) in order to cover a wide range of record lengths. Record selection was constrained (where possible) by event moment magnitude (Mw ≥ 6), nearest distance to fault rupture (D ≥ 20km), and recording station site conditions (NZS1170.5 Class C). This preliminary selection was further refined, according to ground motion scaling and selection criteria outlined in NZS1170.5, producing a suite of 87 DCLS ground motion records. A suite of 54 CALS records was formed by selecting records from the DCLS suite with a scale factor less than or equal to 2 and then amplifying those records by 150% (as per Bridge Manual definition of CALS loading [34]). This method was chosen such that the maximum scaling applied was less than or equal to 3 and thus coherent with the scaling rules of NZS1170.5. The 5-95% significant duration (Ds) definition was used to define record length. Short duration motions were defined as having a Ds ≤ 40s, whilst, long duration motions were defined as having a Ds > 40s. Fig. 1 presents a histogram of the duration of the records used in the DCLS and CALS ground motion suites.

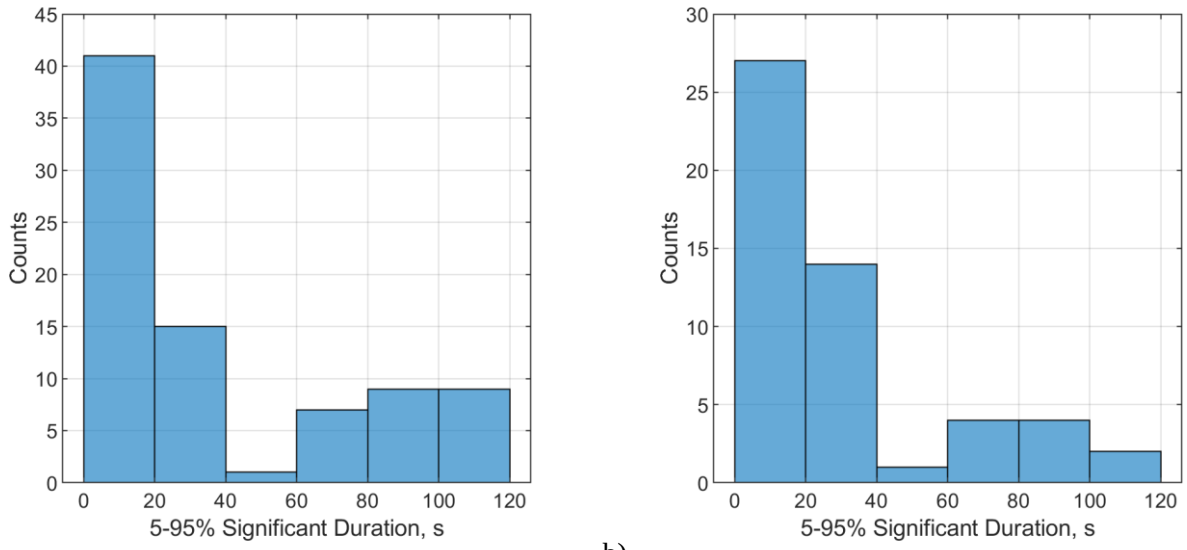

a) b)

Figure 1 - Histogram of the duration of the ground motion records used in a) the DCLS ground motion suite and b) the CALS ground motion suite.

3.4 Models and modelling approach

The five structures were modelled in 2D using OpenSEES. An explicit approach to modelling the rocking behavior, post-tensioning, and dissipative devices was taken. The rocking interface was modelled using the multi-spring element approach. The dissipative devices were modelled as truss elements using the 'Steel02' material (Giuffré-Menegotto-Pinto model) and 'Fatigue' material. The post-tensioning was also modelled as a truss element using the 'Steel01' (Bi-linear model) material calibrated off the material properties of Macalloy bar and used the 'Initial Strain' material to apply the initial post-tensioning force. In series with the post-tensioning was a compression only element which prevented the post-tensioning from going into compression if losses due to yielding exceeded the initial post-tensioning force.

3.4.1 Low cycle fatigue modelling

Low cycle fatigue was included by use of the 'Fatigue' material applied to the dissipaters. $E0 was calculated using Eq. (3) and corresponds to the strain at which one cycle will cause failure. In this study the constants used were m = -0.5 and ε'_0=0.13. The value of the exponent m corresponds to what was proposed by Mander [24] for reinforcing steels. Using this exponent value, ε'_0 was calibrated based off tests conducted by Liu [2] on the four grooved dissipater made from mild steel. Although the value of ε'_0 chosen is higher than the value

reported by Mander [24], it is still conservative in the prediction of the LCF life of the specimens tested by Liu [2].

$$\epsilon_0 = 2^{m+1} \cdot \epsilon_0' \tag{3}$$

3. Results

3.1 Damage Control Limit State (DCLS)

The five models were subject to 56 short and 31 long duration motions from the Damage Control Limit State suite. At this limit state, the main metric for measuring satisfactory performance is the maximum LCF related dissipater damage observed in each simulation for each structural model (Fig. 2). The mean damage from short duration motions was found to range between 9-13%, while for long duration motions, the mean damage was found to range between 22%-37% (Table 3). It is evident that the median and mean values of LCF related damage due to long duration motions are consistently higher than that caused by short duration motions (Fig. 2 and Table 3). This result is consistent with findings from other researchers. The mean amount of LCF damage due to long duration motions was found to range from 180% to 410% more than the mean damage caused by short duration motions. More interestingly the difference in demand between long duration and short duration motions appears to be related to the effective period of the structure (Table 3), where, the difference is greater for short effective period structures. This makes sense as within a given duration of time, more cycles of high frequency shaking can fit than low frequency shaking resulting in higher cyclic demands for short period structures. This can be seen visually in Fig. 5a where the response history of model 1a and 3c are compared against a record acceleration trace.

Although it is clear that longer duration motions cause more damage than short duration motions, the range of damage values due to long duration motions were found to be more spread than those caused by short duration motions (Fig. 2 and Table 3). Furthermore, this range in damage values also seems to reduce with increasing effective period of the model (Fig. 2 and Table 3). The range in observed maximum LCF damage for short duration motions appears to remain relatively consistent over the range of periods of the models.

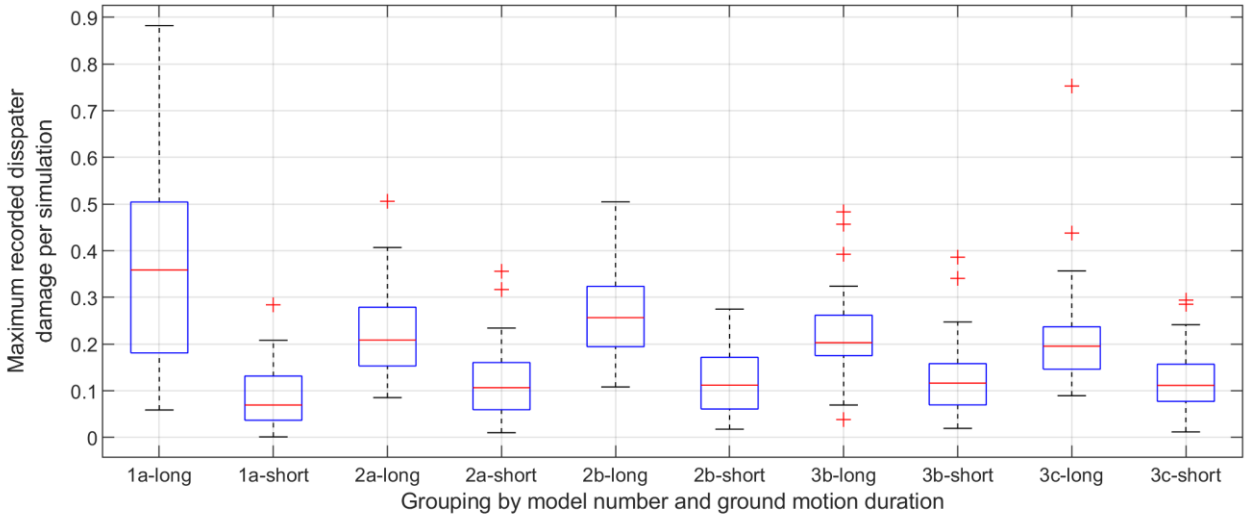

Figure 2: Box and whisker plots indicating the range, 25th and 75th percentiles and median of the maximum recorded dissipater damage observed per simulation. Data points considered as outliers are plotted as '+'.

Table 3 - Comparison of the median values for maximum recorded dissipater damage between short and long duration motions for each model.

		Design				
		1a	2a	2b	3b	3c
Effective period, s		0.76	0.96	1.27	1.58	2.07
Mean of the maximum recorded--dissipater damage per simulation	Short dur.	0.09	0.12	0.12	0.13	0.12
	Long dur.	0.37	0.23	0.26	0.22	0.22
Ratio	Long/short	4.1	1.9	2.2	1.7	1.8
75th Percentile	Short sur	0.13	0.16	0.17	0.16	0.16
	Long dur	0.50	0.28	0.32	0.26	0.24

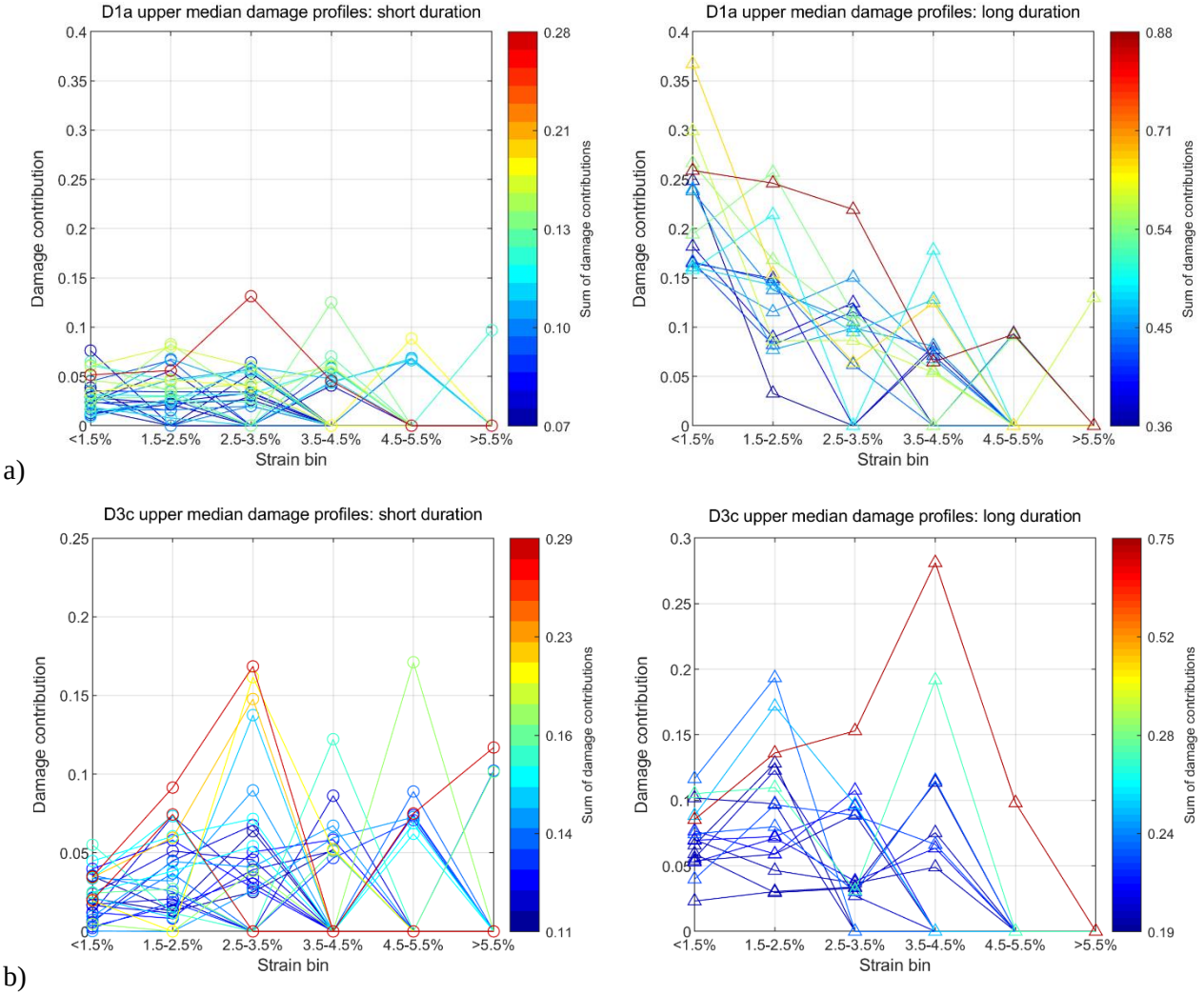

a)

b)

Figure 3: Dissipater damage disaggregated by contribution from binned tensile strains and separated by ground motion duration. Line colour indicates total level of damage received, with warmer colours indicating a higher level of total damage. The data presented corresponds only to simulations for a) model 1a and b) model 3c where the maximum dissipater damage exceeded the median values indicated in Figure 2.

Using the concept of the Palmer-Milgren damage rule, one can determine how much LCF damage received by a dissipater is actually due to it cycling at its design strain. In this study, damage contributions were lumped by strain bins (Fig. 3) and the bin containing the design strain ranged from 4.5% to 5.5% strain. It was found that the highest contribution to total damage was not from the dissipater cycling at its design strain. In fact, generally speaking, the results plotted in Fig. 3 show that between motions there does not appear to be a particular strain bin where the dissipaters appear to receive most of their damage. Moreover, the damage contribution does not appear to be uniformly distributed over multiple strain bins and does not follow any particular shape irrespective of whether the total damage is low or high (i.e. a cool coloured line scaled so that the sum of the damage contributions from each strain bin is increased would look identical to a warm coloured line in Fig. 3). Comparing the damage contributions from long and short duration motions (Fig. 3) it appears that long duration motions cause more total damage by increased cycling at lower level strains (<2.5%). For the short period model 1a this is effect is quite pronounced while for the long period model 3c it is less so.

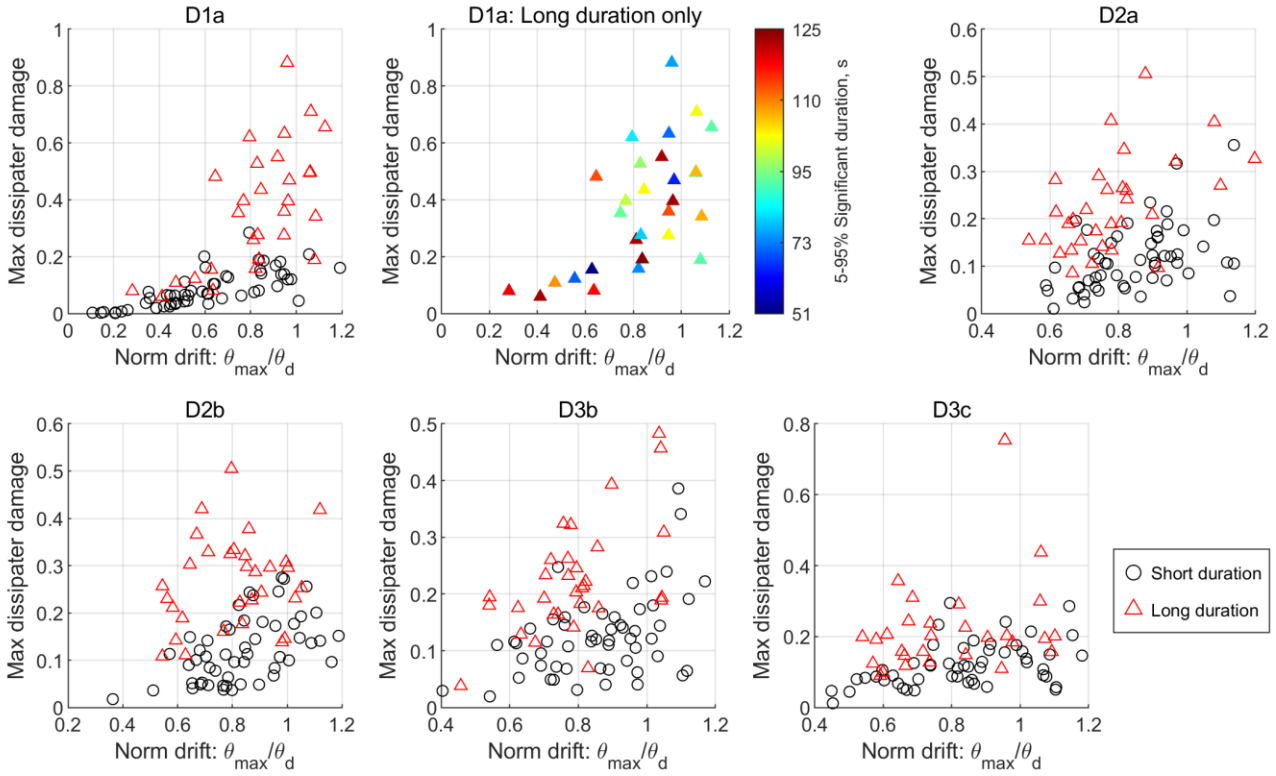

Figure 4: Plots of max dissipater damage vs normalised drift for each model. Data in each plot has been coloured to distinguish results from use of long and short duration records. Top middle plot dissagregates damage from long duration records by record duration using different colours for the markers. Warmer colours indicate results from motions of longer significant duration.

Because LCF damage is strain dependent and dissipater strain depends on the drift of the structure it follows that damage would be correlated to the peak drift reached. Thus, being rigorous in comparing damage from long and short duration motions Fig. 4 presents the same damage data from Fig. 2 plotted against the peak drift reached. For model 1a it is clear that for simulations where the peak drift reached was close to the design drift, long duration motions caused far more damage than short duration motions. This difference in damage seems reduce as the effective period of the model increases (models 2a through to 3c) which is congruent with Fig. 2. Disaggregating the dissipater damage received by model 1a due only to long duration motions by significant period (Fig. 4 top-centre) it is clear that LCF damage is not directly proportional to duration i.e. a longer long duration ground motion does not necessarily mean higher LCF related damage.

In terms of whether there is a clear trend between damage and duration Fig. 5b presents a scatter plot of damage as a function of duration only for simulations where the maximum drift reached was between 80-120% of the design drift θ_d. Fig. 5b shows that long duration motions cause more damage than short duration motions, but, that the correlation between the two is weak due to significant scatter in possible damage caused by a ground motion of given duration. The authors believe that this weak correlation tells us that other property(s) of ground motions must be accounted for as duration alone cannot explain the level of LCF damage a given ground motion will cause.

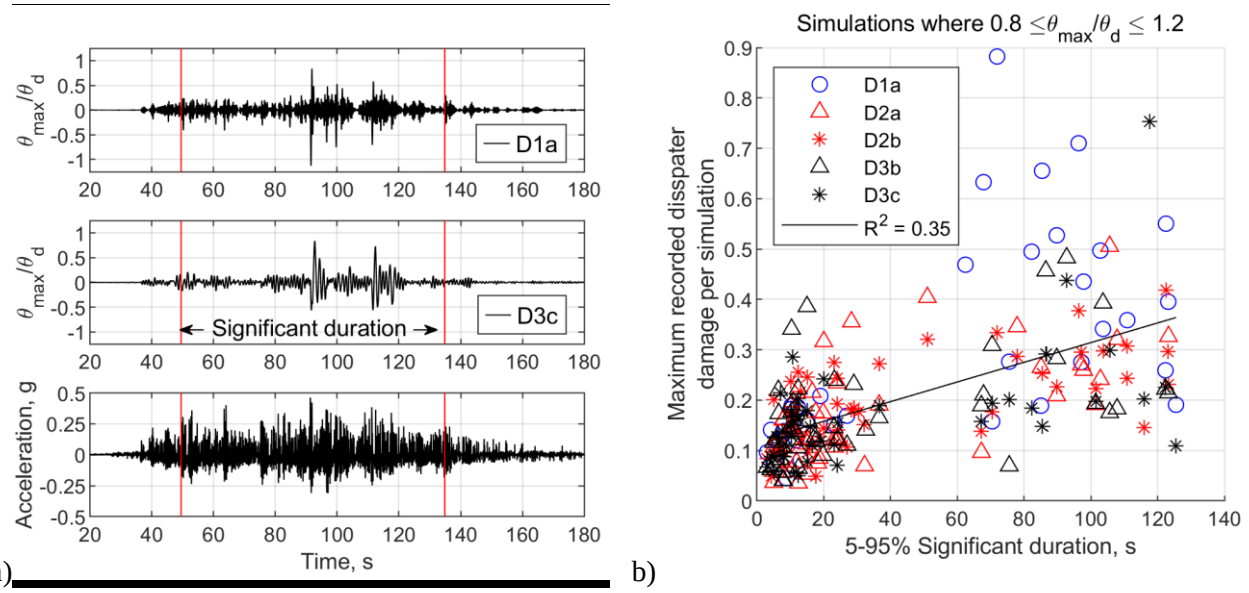

a) b)

Figure 5: a) Comparison of normalised drift traces for designs 1a and 3c with the acceleration trace of the Tohoku Earthquake measured at station FKS006 N-S component. The 5-95% significant duration is annotated. b) Scatter plot of maximum LCF related damage against ground motion duration for all models. The data plotted is only from simulations where the maximum drift reached is within 0.8 to 1.2 times the design drift.

3.2 Collapse Avoidance Limit State (CALS)

At the Collapse Avoidance Limit State, dissipater fracture is expected. However, the number of fractures should be limited such that the total loss in hysteretic damping and moment capacity does not result in excessive displacements leading to collapse of the structure. The CALS suite consisted of 41 short duration motions and 13 long duration motions. Results from simulations where the model did not exceed 120% of the DCLS displacement or exceeded 150% of the expected CALS displacement prior to first dissipater fracture were discarded. This resulted in varying numbers of "successful" short and long duration motion results presented in the Fig. 6. For most of the models about 37% of the long duration motions resulted in dissipater rupture (Fig. 6a). Model 3b is an exception to this where only about 20% of long duration motions caused rupture. (Fig. 6a) With respect to short duration motions, about 27% of these resulted in dissipater rupture. Short duration CALS level motions did not result in LCF related dissipater rupture (Fig. 6a) for model D1a. It was found that the peak drift reached in the simulations for each model occurred more often (about 50% more) after fracture of the first dissipater had occurred.

Investigating the relationship between the percentage of dissipater layers fractured, normalized drift, and ground motion duration (Fig. 6b), model 3b tended to lose the most layers of dissipaters due to LCF. Three simulations where all of the layers of dissipaters fractured resulted in the models exceeding the expected CALS drift by over 200%. The average number of dissipater layers fracturing due to LCF was found to be 46%. From the duration correlated color coding of the markers in Fig. 6b it is clear that there is poor correlation between duration and number of dissipater layers expected to fail due to LCF.

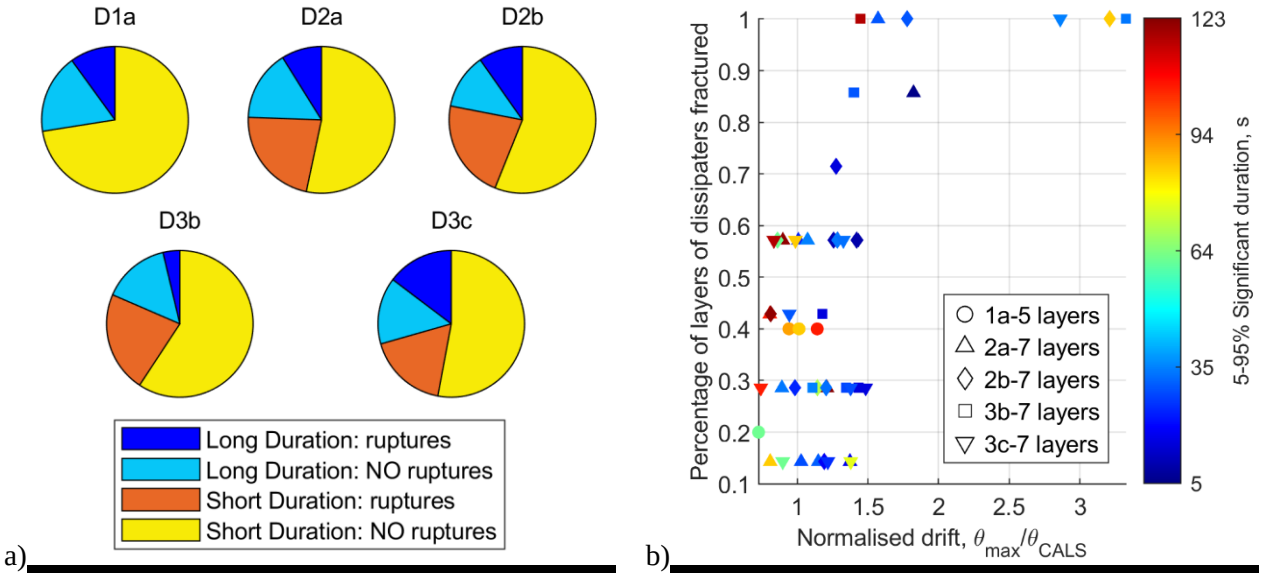

Figure 6 - a) pie charts showing proportion of long and short duration motions which resulted in either rupture or no rupture of dissipaters. b) Scatter plot of percentage of fractured dissipater layers as a function of normalised peak drift. Marker shapes indicate structural model and marker colour indicates ground motion significant duration.

3. Conclusion

The choice of design strain for metal components intended for hysteretic energy dissipation does not appear to be a straightforward question to answer. This issue was investigated in this paper by response history analysis of five post-tensioned rocking bridge pier models subject to a suite of design limit state (ULS) and beyond design limit state (MCE) scaled ground motions. Particular focus was given towards using a suite of motions representing a large range of significant durations. The dissipaters used in the models were designed to reach 5% strain, as per the PRESSS handbook, at the pier design displacement and used values of low cycle fatigue properties that can be considered typical for mild steel. Broadly speaking it was found that, 5% design strain appears to be a reasonable value to use from the perspective of low cycle fatigue (LCF) capacity considering a single ULS level ground motion. However, at MCE, it is concerning the peak drift reached after loss of a few layers of dissipaters. Another concern, is the extreme range of LCF damage which can be caused by long duration ULS level motions. It was found that the mean and range of damage caused by long duration motions are dependent on the effective period of the structure and appear to be largest for structures of short effective period. In this study was found that up to 88% of the LCF life of the dissipaters in a short period bridge pier could be consumed at the ULS. This is in contrast to a maximum of 20% under a short duration motion. The majority of the contribution to total LCF damage was found not to be caused by cycling at the design strain. Furthermore, the results indicate that damage contribution as a function of cycling within particular strain bins appears to be random. It was found that long duration motions cause more LCF damage than short duration motions at both ULS and MCE. However, the direct correlation between duration and expected LCF damage was found to be weak due to significant scatter in observed LCF damage. This finding suggests that duration alone is not enough to tell us how much LCF damage would be expected due to a given ground motion. Furthermore, the findings suggest that selection of design strain should be made based on expected ground motion duration, effective period of the structure, and consideration of multiple/subsequent earthquake events.

6. References

[1] F. Sarti, A. Palermo, and S. Pampanin, "Fuse-Type External Replaceable Dissipaters: Experimental Program and Numerical Modeling," *J. Struct. Eng.*, vol. 142, no. 12, 2016.

[2] R. Liu and A. Palermo, "Characterization of a filler free buckling restrained fuse type energy dissipation device for seismic applications," *J. Struct. Eng.*, vol. Forthcomin, 2020.

[3] W. C. Stone, G. S. Cheok, and J. F. Stanton, "Performance of Hybrid Moment-Resisting Precast Beam Column Concrete Connections Subjected to Cyclic Loading," *ACI Struct. J.*, vol. 92, no. 2, pp. 229–249, 1995.

[4] M. J. N. Priestley, "The PRESSS Program Current Status and Proposed Plans for Phase III," *PCI J.*, vol. 41, no. 2, pp. 22–40, 1996.

[5] A. Palermo, S. Pampanin, and G. M. Calvi, "Concept and development of hybrid solutions for seismic resistant bridge systems," *J. Earthq. Eng.*, vol. 9, no. 6, pp. 899–921, 2005.

[6] S. Motaref, M. S. Saiidi, and D. H. Sanders, "Shake table studies of energy-dissipating segmental bridge columns," *J. Bridg. Eng.*, vol. 19, no. 2, pp. 186–199, 2014.

[7] J. B. Mander and C. T. Cheng, "Seismic resistance of bridge piers based on damage avoidance design," National Center for Earthquake Engineering Research, New York, NCEER-97-0014, 1997.

[8] W. Trono, G. Jen, M. Panagiotou, M. Schoettler, and C. P. Ostertag, "Seismic Response of a Damage-Resistant Recentering Posttensioned-HYFRC Bridge Column," *J. Bridg. Eng.*, vol. 20, no. 7, 2015.

[9] M. A. ElGawady and A. Sha'lan, "Seismic Behavior of Self-Centering Precast Segmental Bridge Bents," *J. Bridg. Eng.*, vol. 16, no. 3, pp. 328–339, 2011.

[10] J. Wang, Z. Wang, Y. Tang, T. Liu, and J. Zhang, "Cyclic loading test of self-centering precast segmental unbonded posttensioned UHPFRC bridge columns," *Bull. Earthq. Eng.*, vol. 16, no. 11, 2018.

[11] C. Christopoulos, A. Filiatrault, C. M. Uang, and B. Folz, "Posttensioned Energy Dissipating Connections for Moment-Resisting Steel Frames," *J. Struct. Eng.*, vol. 128, no. 9, pp. 1111–1120, 2002.

[12] G. Deierlein *et al.*, "Earthquake resilient steel braced frames with controlled rocking and energy dissipating fuses," *Steel Constr.*, vol. 4, no. 3, pp. 171–175, 2011.

[13] F. Sarti, A. Palermo, and S. Pampanin, "Quasi-Static Cyclic Testing of Two-Thirds Scale Unbonded Posttensioned Rocking Dissipative Timber Walls," *J. Struct. Eng.*, vol. 142, no. 4, 2016.

[14] A. Iqbal, S. Pampanin, and A. Buchanan, "Seismic Performance of Full-Scale Post-Tensioned Timber Beam-Column Connections," *J. Earthq. Eng.*, vol. 20, no. 3, 2016.

[15] S. Pei *et al.*, "Experimental Seismic Response of a Resilient 2-Story Mass-Timber Building with Post-Tensioned Rocking Walls," *J. Struct. Eng.*, vol. 145, no. 11, 2019.

[16] G. W. Rodgers *et al.*, "Performance of a damage- protected beam-column subassembly utilizing external HF2V energy dissipation devices," *Earthq. Eng. Struct. Dyn.*, vol. 37, no. 13, pp. 1549–1564, 2008.

[17] B. G. Morgen and Y. C. Kurama, "A Friction Damper for Post-Tensioned Precast Concrete Beam-To-Column Joint," in *13th World Conference on Earthquake Engineering*, 2004, no. 3189.

[18] W. Y. Kam, S. Pampanin, A. Palermo, and A. J. Carr, "Self-centering structural systems with combination of hysteretic and viscous energy dissipations," *Earthq. Eng. Struct. Dyn.*, vol. 39, no. 10, pp. 1083–1108, 2010.

[19] S. White, "Controlled damage rocking systems for accelerated bridge construction," University of

Canterbury, 2014.

[20] A. Mohebbi, M. S. Saiidi, and A. M. Itani, "Shake Table Studies and Analysis of a PT-UHPC Bridge Column with Pocket Connection," *J. Struct. Eng.*, vol. 144, no. 4, p. 04018021, 2018.

[21] H. Roh and A. M. Reinhorn, "Hysteretic behavior of precast segmental bridge piers with superelastic shape memory alloy bars," *Eng. Struct.*, vol. 32, no. 10, pp. 3394–3403, 2010.

[22] A. El-Bahy, S. K. Kunnath, W. C. Stone, and A. W. Taylor, "Cummulative Seismic Damage of Circular Bridge Columns: Benchmark and Low-Cycle Fatigue Tests," *ACI Struct. J.*, vol. 96, no. 4, pp. 633–641, 1999.

[23] A. El-Bahy, S. K. Kunnath, W. C. Stone, and A. W. Taylor, "Cummulative Seismic Damage of Circular Bridge Columns: Variable Amplitude Tests," *ACI Struct. J.*, vol. 96, no. 5, pp. 711–719, 1999.

[24] J. B. Mander, F. Panthaki, and A. Kasalanati, "Low-Cycle Fatigue Behavior of Reinforcing Steel," *J. Mater. Civ. Eng.*, vol. 6, no. 4, pp. 453–468, 1994.

[25] P. Uriz and S. A. Mahin, "Toward Earthquake-Resistant Design of Concentrically Braced Steel-Frame Structures," Berkley, California, 2008/08, 2008.

[26] J. Brown and S. K. Kunnath, "Low-Cycle Fatigue Failure of Reinforcing Steel Bars," *Mater. J.*, vol. 101, no. 6, pp. 457–466, 2004.

[27] G. W. Zhang, Y. Xiao, and S. K. Kunnath, "Low-Cycle Fatigue Damage of Circular Concrete-Filled-Tube Columns," *ACI Struct. J.*, vol. 106, no. 2, pp. 151–159, 2009.

[28] A. Teran-Gilmore and J. O. Jirsa, "A Damage Model for Practical Seismic Design that Accounts for Low Cycle Fatigue," *Earthq. Spectra*, vol. 21, no. 3, pp. 803–832, 2005.

[29] R. Chandramohan, J. W. Baker, and G. Deierlein, "Quantifying the influence of ground motion duration on structural collapse capacity using spectrally equivalent records," *Earthq. Spectra*, vol. 32, no. 2, pp. 927–950, 2016.

[30] M. Mohammed, D. H. Sanders, and I. G. Buckle, "Reinforced concrete bridge columns tested under long and short-duration ground motions," in *16th World Conference on Earthquake Engineering*, 2016.

[31] J. Hancock and J. J. Bommer, "Using spectral matched records to explore the influence of strong-motion duration on inelastic structural response," *Soil Dyn. Earthq. Eng.*, vol. 27, no. 4, pp. 291–299, 2007.

[32] D. Marriott, S. Pampanin, and A. Palermo, "Biaxial testing of unbonded post-tensioned rocking bridge piers with external replacable dissipaters," *Earthq. Eng. Struct. Dyn.*, vol. 40, no. 15, pp. 1723–1741, 2011.

[33] C.-L. Wang, Y. Liu, and L. Zhou, "Experimental and numerical studies on hysteretic behavior of all-steel bamboo-shaped energy dissipaters," *Eng. Struct.*, vol. 165, pp. 38–49, 2018.

[34] New Zealand Transport Agency, *Bridge manual 3rd Edition*, 3rd ed. 2013.

